Journal of Magnetism and Magnetic Materials 345 (2013) 276–281

Contents lists available at SciVerse ScienceDirect

Journal of Magnetism and Magnetic Materials

journal homepage: www.elsevier.com/locate/jmmm

Synthesis and characterization of nanocrystalline $Ni_{0.94}Co_{0.03}Mn_{0.04}Cu_{0.03}Fe_{1.96-x}Al_xO_4$ ferrites for microwave device applications

T. Ramesh [a], R.S. Shinde [b], S.R. Murthy [a,*]

[a] Department of Physics, Osmania University, Hyderabad, India
[b] Ferrite Laboratory, RRCAT, Indore, India

ARTICLE INFO

Article history:
Received 4 May 2013
Received in revised form
7 June 2013
Available online 4 July 2013

Keywords:
Ferrites
Microwave hydrothermal method
Magnetic properties
Dielectric properties

ABSTRACT

Nanocrystalline $Ni_{0.94}Co_{0.03}Mn_{0.04}Cu_{0.03}Fe_{1.96-x}Al_xO_4$ ($x=0$, 0.1, 0.3, 0.5, 0.7 and 0.9) were synthesized using the microwave hydrothermal method at 160 °C/40 min. The synthesized powders were characterized using X-ray diffraction (XRD), Transmission electron microscopy (TEM) and Fourier transform infrared spectra (FTIR). The nanopowders were densified using microwave sintering method at 950 °C/30 min. The prepared samples were characterized using XRD and Field emission scanning electron microscopy (FESEM). The substitution of nonmagnetic Al^{3+} ions in place of magnetic Fe^{3+} ions results decrease of the density and lattice constant. An increase in dc resistivity and reduction in the initial permeability, saturation magnetization (M_s) and Curie temperature (T_C) has been observed with a substitution of Al^{3+} ions. High dc resistivity and low dielectric, magnetic losses combined with an excellent temperature stability of magnetization ($4\pi M_s$) observed in the present ferrites can be explored for the fabrication of microwave device such as circulators, phase shifters etc.

1. Introduction

Polycrystalline ferrites have been regarded as good magnetic and dielectric materials. Their physical properties depend on many factors like preparation method, chemical composition, sintering temperature and time, type of substitutions and distribution of cations among tetrahedral and octahedral sites [1]. Out of all the soft ferrites, Al^{3+} substituted nickel ferrites were suitable for microwave devices, because they possess a high electrical resistivity and low eddy current losses with low dielectric and magnetic losses [2–6]. Keeping this in view, we have selected Al^{3+} substituted nickel ferrites and small amounts of Co^{2+}, Cu^{2+} and Mn^{3+} ions were added. The Co^{2+} ions were added to increase the spin wave width of Ni ferrite system which increases the power handling capability [5]. In order to improve the density of Ni ferrite, small amount of Cu^{2+} was added to it. A small amount of Mn^{3+} has been added to Ni ferrite to reduce the dielectric losses and to control magnetostriction coefficient [6]. Thus, nanocrystalline $Ni_{0.94}Co_{0.03}Mn_{0.04}Cu_{0.03}Fe_{1.96-x}Al_xO_4$ ($x=0$, 0.1, 0.3, 0.5, 0.7 and 0.9) were synthesized using the microwave hydrothermal method and characterized using XRD and TEM. As synthesized nano size powders were densified using the microwave sintering method. The electrical and magnetic properties were carried out.

2. Experimental method

Pure nickel nitrate [Ni $(NO_3)_2 \cdot 6H_2O$], cobalt nitrate [Co $(NO_3)_2 \cdot 6H_2O$], manganese nitrate [Mn $(NO_3)_3 \cdot 9H_2O$], copper nitrate [Cu $(NO_3)_2 \cdot 6H_2O$], aluminum nitrate [Al $(NO_3)_3 \cdot 6H_2O$] and ferric nitrate [Fe $(NO_3)_3 \cdot 9H_2O$] were measured according to their stoichiometric proportions and dissolved in 100 ml of deionized water to obtain final composition $Ni_{0.94}Co_{0.03}Mn_{0.04}Cu_{0.03}Fe_{1.96-x}Al_xO_4$ (where $x=0$ (AS1), 0.1 (AS2), 0.3 (AS3), 0.5 (AS4), 0.7 (AS5) and 0.9 (AS6)). An aqueous NaOH (4 M) solution was added to this mixture until the desired pH=~9.5 value was obtained. Then the mixture was transferred into a Teflon lined vessel and treated using a microwave digestion system (Model MDS-2000, CEM Corp., Mathews, NC) at 160 °C/40 min [7–10]. The products obtained were filtered and washed repeatedly with deionized water followed with ethanol to remove the residual nitrates present in the final compound. The final slurry was dried overnight at 60 °C. The synthesized powders were characterized using powder XRD (Philips PW-1730 X-ray diffractometer with Cu-K_α radiation ($\lambda=1.5406$ A°), TEM (model JEM-2010, JEOL, Tokyo, Japan) and FTIR (FTIR, Brucker tensor 27). The as prepared nanopowders were granulated using 2 wt% polyvinyl alcohol as a binder. Then the powders were uniaxially pressed at a pressure of 150 MPa to form pellet (8 mm Diameter, 2 mm Height) and toroidal (ID 4 mm, OD 9 mm) specimens. After the binder was burnt out at 300 °C, the compacts were microwave sintered at

* Corresponding author.
E-mail address: ramanasarabu@gmail.com (S.R. Murthy).

0304-8853/$ - see front matter © 2013 Elsevier B.V. All rights reserved.
http://dx.doi.org/10.1016/j.jmmm.2013.06.041

950 °C/30 min in the air. The final sintering temperature 950 °C was chosen after the detailed study of sintering temperature on density by specially designed microwave oven [11]. The sintered samples were characterized by XRD and SEM (Model JEOL, Tokyo, Japan).

Initial permeability and dielectric constant have been measured at 1 MHz on all the ferrites using an LCR meter (Kokuyo Electric Co., Japan model no.KC-605). The dc electrical resistivity (ρ_{dc}) of the samples was measured using two probe method at room temperature. Magnetic properties such as saturation magnetization (M_S) and coercivity (H_C) were obtained from recorded hysteresis loops using the Vibration Sample Magnetometer (VSM, Model DMS 1660). Temperature dependent magnetization studies were conducted in the range of room temperature to the Curie temperature (T_C) using a pulsed magnetometer with a maximum applied field of 2 Tesla.

2.1. Results and discussions

Fig. 1 shows powder X-ray diffraction patterns for all the as synthesized powders. It can be seen from the figure that the XRD patterns are essentially a single phase with no additional peaks or phases including unrequited oxides or impurities. A closer inspection of the XRD patterns reveals that the peak intensities have become more broader with an increase of Al^{3+} substitution. This may be due to the substitution of Al^{3+} ions in place of Fe^{3+} ions which lowers the crystallite size. The average particle size for each composition has been calculated using the Scherrer formula: $D_m = K\lambda/\beta\cos\theta$, where K (shape factor) is a constant, β is the full width half maxima, λ is the wavelength of X-ray (1.5406 Å) used and θ is the diffraction angle. The average values of crystallite size

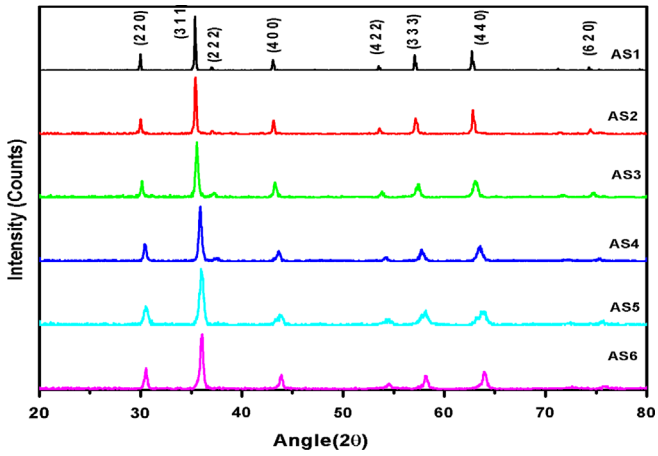

Fig. 1. XRD patterns for as-synthesized nanocrystalline NiCoMnCu Al ferrites.

obtained from XRD patterns are given in Table 1. It can be observed from the table that the crystallite size decreases from 34 nm to 15 nm with an increase of Al^{3+} substitution. Similar result has been observed in Ni–Al ferrite system [12,13].

TEM pictures for three typical as synthesized ferrite powders are shown in Fig. 2. The selected area diffraction (SAD) patterns of these specimens reveal the formation of single phase polycrystalline ferrites. No trace of an impurity or undesirable phase was detected in any of the ferrite. The diffraction rings, characteristic of nanocrystalline aggregates, have been indexed and obtained values of particle size are presented in Table 1. Occasional spots in the SAD pattern may arise from coarse crystallites or agglomerates. It may be noted that the observed average particle sizes from TEM picture are nearly same as that calculated from XRD peak broadening. The specific surface area (S) has been measured using Quantasorb equipment (Quantachrome Corp.) by BET technique and the results are presented in Table 1. It can be seen from the table that the S increases with the decrease in particle size.

Fig. 3 shows FTIR spectra for all as synthesized powders. It can be observed from the figure that two prominent peaks around 574 and 420 cm^{-1} represent that of Fe–O stretching vibrations in the tetrahedral (A) and octahedral (B) lattices. The tetrahedral peak has been observed at a higher wavelength region as compared to octahedral peak in the spectra. More energy is required to vibrate the bond because of the Fe–O vibration bond in the tetrahedral lattice has a shorter bond length when compared to octahedral lattice. It can be seen from the figure that a shift is observed in the position of the Fe–O octahedral and tetrahedral peaks in the samples AS1–AS6. The shifting of bands wave number towards the high frequency side is attributed to the decrease in the unit cell dimension. The increase in the frequency of the absorption bands is attributed to the creation of lattice vacancies. These vacancies are due to the vibration of octahedral and tetrahedral groups [14,15].

Fig. 4 shows the XRD patterns for the microwave sintered ferrite samples ($x=0$ (MS1), 0.1 (MS2), 0.3 (MS3), 0.5 (MS4), 0.7 (MS5) and 0.9 (MS6)). The pattern shows the formation of single phase cubic spinel structure without any sign of secondary phase. In ferrites the intensities of (220) and (422) peaks are sensitive to presence of cations in tetrahedral (A) sites and (222) peak is sensitive to octahedral (B) sites. The intensity of the (511)/(333) peak is related to the oxygen content in the sample [16,17]. The patterns also indicated that the peak intensities of (220), (422) and (222) decrease with an increase of Al^{3+} substitution. This indicates that both A and B sites are affected by the substitution of Al^{3+}.

The average grain size was calculated using Scherrer formula and obtained results are presented in Table 2. It can be seen from the table that the grain size for microwave sintered samples are in the nanocrystalline (<100 nm) range. Lattice parameter (a) was calculated using the equation: $a=\lambda(h^2+l^2+k^2)^{1/2}/2\sin\theta$, where λ is the wavelength of X-ray radiation, θ is the Bragg angle and (h, k, l)

Table 1
Preparation data on Al substituted NiCoCuMn ferrites.

As synthesized samples				Sintered samples						
Sample	**Crystallite size from XRD (nm)**	**Particle size from TEM (nm)**	**S (m^2/g)**	**Sample**	**Sintered samples lattice constant (Å)**	**Bulk density (g/cc)**	**X-ray density (g/cc)**	**Porosity (%)**	**Grain size from XRD (nm)**	**Grain size from FESEM (nm)**
AS1	34	35	33	MS1	8.3713	5.10	5.31	4	79	87
AS2	31	32	36	MS2	8.3676	4.98	5.25	5	74	83
AS3	27	26	45	MS3	8.3196	4.92	5.21	6	69	79
AS4	21	23	53	MS4	8.2957	4.76	5.12	7	65	76
AS5	18	20	62	MS5	8.2746	4.61	5.02	8	62	73
AS6	16	18	70	MS6	8.2411	4.58	4.95	8	59	69